Journal of Climate Change
ISSN 2395-7611 Volume 12 (2026) No. 2. pp. 325–336

https://doi.org/10.70917/jcc-2026-019
Article

Evolution Characteristics of Extreme Precipitation in Northern China: A Case Study of Chaohu Lake Basin

Ye Zhang [1], Leizhi Wang [1,*], Dan Tian [2], Wei Zhu [3], Lei Wu [4], Pengxin Deng [5] and Jianwen Hu [1]

1 State Key Laboratory of Hydrology-Water Resources and Hydraulic Engineering, Nanjing Hydraulic Research Institute, Nanjing Jiangsu, 210029, China; work_yzhang@163.com(ZHANG Ye); wanglz@nhri.cn (WANG Leizhi); jianwen_hu@tju.edu.cn(HU Jianwen)
2 China Three Gorges Corporation, Wuhan Hubei, 430014, China; tian_dan3@ctg.com.cn(TIAN Dan)
3 Hunan Provincial Water Conservancy and Hydropower Survey and Design Institute, Changsha Hunan, 410007, China; 18890024753@163.com(ZHU Wei)
4 Key Laboratory of Flood & Drought Disaster Defense, the Ministry of Water Resources, Nanjing Jiangsu, 210029, China; School of Resources and Environment, Anhui Agriculture University, Hefei Anhui, 230036 China; wulei@ahau.edu.cn(WU Lei)
5 Bureau of Hydrology, Changjiang Water Resources Commission, Wuhan Hubei, 430010, China; dpx_work@163.com(DENG Pengxin)
* Correspondence author: wanglz@nhri.cn

Abstract: Under the background of global climate change, extreme precipitation events are becoming more frequent in the monsoon region of northern China. The Chaohu Lake Basin, as a typical transitional zone in the middle and lower reaches of the Yangtze River, has a precipitation variability that is simultaneously influenced by the interaction between the ocean and the atmosphere and the expansion of the Hefei metropolitan area. Based on daily precipitation data from 15 meteorological stations, this study aims to investigate the spatiotemporal patterns and drivers of extreme precipitation in the basin from 1961 to 2019 by constructing a "Trend-Mutation-Probability (TMP)" three-dimensional analysis framework. Results show: 1) The annual average precipitation in the Chaohu Lake Basin shows a significant upward trend (2.4 mm/yr, $p < 0.05$), with a more significant increase at the edge stations (such as station 15 reaching 5.1 mm/yr); 2) The year of the precipitation mutation point is 1979 ($H = 0.52$), and after the mutation, the 90th percentile ($P=0.9$) precipitation increases by 154.6 mm; 3) The PRCPTOT index shows the most significant growth (2.4 mm/yr), and the frequency of extreme events significantly increases. This study not only presents the novel TMP diagnostic framework for broader application but also delivers specific, actionable insights for updating flood risk management policies and infrastructure design standards in the densely populated Yangtze River Delta, thereby strengthening the region's climate resilience.

Keywords: Chaohu Lake Basin; extreme precipitation; mutation diagnosis; probability distribution

1. Introduction

Climate change and human activities are two main forces that influence the hydrological cycle processes in river basins (Wu et al., 2024; Tang, 2020). In recent years, the precipitation pattern in the northern regions of China has undergone significant changes(Tysa, 2025). Understanding the evolution of meteorological elements in river basins is crucial. It is fundamental to unraveling the mechanisms of the hydrological cycle and improving the management of flood control and drainage infrastructure.

Global precipitation patterns have undergone notable changes, prompting extensive research by scholars worldwide. For instance, Zhang et al. (2023) systematically analyzed global precipitation trends using Integrated Multi-satellite Retrievals for Global Precipitation Measurement (GPM) data, concluding that global precipitation exhibits a significant increasing trend overall, with more pronounced increases in winter and spring compared to summer and autumn. Xing et al. (2019) examined global daily precipitation variations based on Climate Prediction Center MORPHing technique(CMORPH) precipitation data and found that the highest daily precipitation occurs over continental regions near the equator, with significant differences in precipitation changes between oceans and land. Du Junkai et al. (2023) employed trend analysis and mutation tests to study precipitation evolution in China, revealing an overall increase in the concentration of annual precipitation distribution. Xu Xiaolu et al. (2024) analyzed variations in different precipitation intensity levels across China, noting a decreasing trend in light rain days but an increasing trend in moderate-to-heavy rain days, with precipitation intensity gradually weakening from southeast to northwest.

Moreover, numerous studies highlight that under the influence of climate change and human activities, extreme precipitation events are becoming more frequent and intense (Franzke, 2022; Zhao et al, 2024). In February 2022, the Intergovernmental Panel on Climate Change (IPCC) Sixth Assessment Report (AR6), Climate Change 2022: Impacts, Adaptation, and Vulnerability (IPCC, 2022) warned that under current climate trends, extreme events will grow more frequent and severe, potentially pushing ecosystems toward irreversible tipping points. Du et al. (2022) analyzed the frequency of extreme precipitation consecutive days (EPCD) using observational and multi-model datasets, finding that EPCD is increasing in most land regions and will further rise with continued global warming. Guo et al. (2023) investigated China's extreme precipitation indices under 1.5–2.0°C global warming scenarios (SSP245, SSP370, and SSP585), concluding that higher greenhouse gas emissions and warming levels will lead to more frequent and intense extreme precipitation events in China. Zhang et al. (2023) developed a comprehensive hazard index for extreme climate events in the Yangtze River Basin, revealing an increasing risk of extreme precipitation and low-temperature events, which could exacerbate socioeconomic impacts.

The Chaohu Lake Basin is located in the key transition zone of the East Asian monsoon (117.3°E - 118.9°E, 30.7°N - 32.2°N). Its precipitation variability is sensitive to both the sea-air interaction (such as ENSO) and human activities (such as the expansion of the Hefei metropolitan area), providing an ideal window for exploring the hydrological extremization under climate-human combined stress. Despite evident changes in precipitation characteristics in the Chaohu Lake Basin, quantitative research on its evolution remains limited. This study analyzes the extreme precipitation evolution in the basin, focusing on extreme precipitation indices, trend analysis, mutation detection, and changes in precipitation distribution before and after mutation points. The paper is structured as follows: (1) Section 2 introduces the study area and data; (2) Section 3 describes the methodology; (3) Section 4 presents results and discussion; and (4) Section 5 provides conclusions.

2. Study Case

2.1. Basin Overview

This study selected the Chaohu Lake Basin in Anhui Province, China as a typical case to explore the evolution characteristics of the water runoff pattern under the background of climate change and its impacts. The Chaohu Lake Basin is located in the key area of the East Asian monsoon and is highly sensitive and reactive to climate change. It is an ideal place for studying the interaction between climate change and hydrological processes. In recent years, this basin has experienced frequent extreme precipitation events, with a distinct 'drought-flood alternation' feature, providing clear empirical evidence for analyzing the regional impact of climate change. As a highly developed typical basin, the intense human activities in the Chaohu area are deeply coupled with the natural climate process, offering a unique perspective for understanding the complex interaction between the human-land system. This research has urgent practical significance for ensuring the water security, food security, and ecological security of the Hefei metropolitan area and Anhui Province. The research results can provide scientific support for the strategic formulation of regional adaptation to climate change.

The study area encompasses the Chaohu Lake Basin (Figure 1), geographically located between 117.3°E–118.9°E and 30.7°N–32.2°N. Situated on the left bank of the lower reaches of the Yangtze River, the basin spans the central part of Anhui Province administratively. Major tributaries include the Hangbu River, Fengle River, and Nanfei River. The terrain is predominantly characterized by plains and low hills, with topography exerting minimal overall influence on precipitation. The mean annual precipitation ranges from 800 to 1400 mm, with rainfall concentrated primarily between June and September.

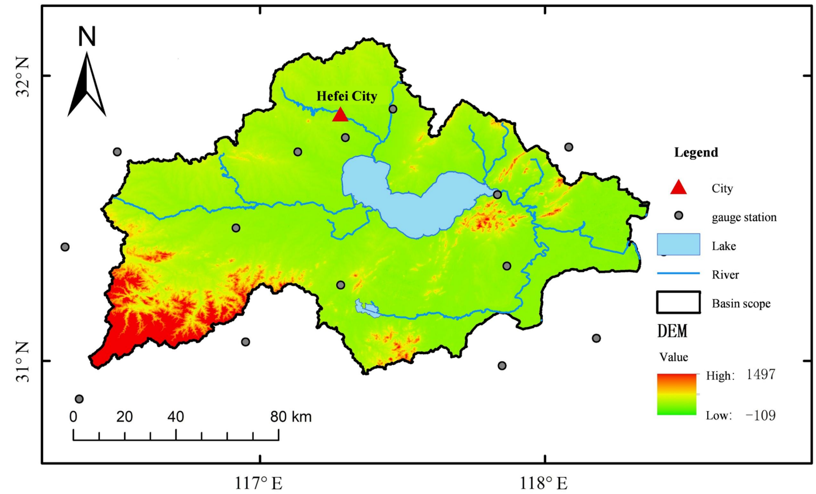

Figure 1. Study area

2.2. Data Sources

Daily ground observation data from 1961 to 2019 were obtained for 15 national meteorological stations within and around the Chaohu Lake Basin from the China Meteorological Data Service Center (http://data.cma.cn), hosted by the National Meteorological Information Center. This set of data has been widely adopted in research conducted in the Chinese region, thereby demonstrating the quality of its data.

3. Research Methods

3.1. The Trend-Mutation-Probability (TMP) Diagnostic Framework

To move beyond conventional descriptive analysis and systematically diagnose the evolution of extreme precipitation, this study proposes a novel Trend-Mutation-Probability (TMP) diagnostic framework (Figure 2). This integrated frameyijigngzaiwenzhongyinyongwork dissects the complex process of hydro-climatic change into three logically sequential dimensions to comprehensively address the what, when, and how of the changes.

Trend Diagnosis: This initial phase quantifies the long-term direction and magnitude of changes in precipitation extremes, answering the question of what is changing. It utilizes a suite of extreme precipitation indices and robust statistical trend analyses.

Mutation Diagnosis: Building on the identified trends, this phase detects potential abrupt change points in the time series, pinpointing when a significant regime shift occurred. It employs a multi-stage diagnostic procedure to ensure reliability.

Probability Diagnosis: The final phase investigates how the statistical properties and risk characteristics of extremes have changed after the mutation, elucidating how the change manifests. It compares probability distributions (e.g., GEV) between pre- and post-mutation periods.

The strength of this framework lies in its systematic logic and generalizability, providing a transferable template for diagnosing hydro-climatic extremes in other regions. The specific methodologies applied within each phase are detailed in the following subsections.

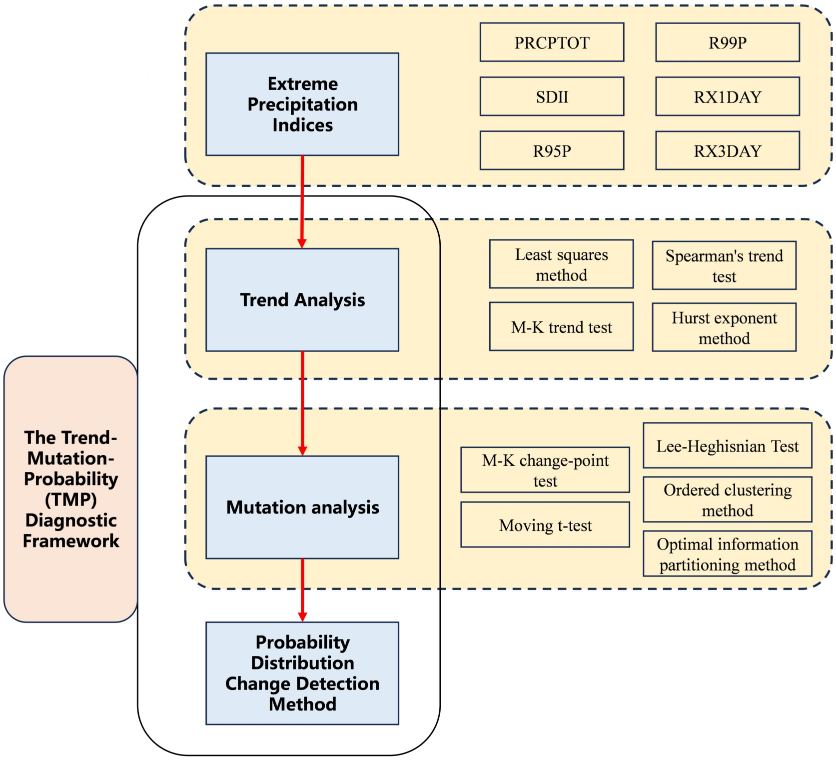

Figure 2. Technical approach

3.2. Extreme Precipitation Indices

Extreme hydrological events primarily include extreme temperatures, extreme precipitation, and extreme runoff. From a probabilistic perspective, extreme events are those with low or very low likelihoods of occurrence. Initially, extreme events were defined based on fixed thresholds—events exceeding or falling below a specific value were classified as extreme. However, due to climatic variations across regions, percentile-based threshold methods have become widely adopted for determining extreme event thresholds (He and Su, 2018).

Currently, the "Climate Change Monitoring and Indices" developed by the Expert Team on Climate Change Detection and Indices (ETCCDI) have been extensively applied in the analysis and research of extreme climate events (Zhang et al, 2024; Teegavarapu and Nayak, 2017; Liu et al, 2017; Ayugi et al, 2021). Considering the geographical location and natural environmental characteristics of the study area, this paper selects six extreme precipitation indices from the 27 ETCCDI climate indices. The definitions of these indices are detailed in Table 1. This study does not involve human participants, personal data or any form of interpersonal interaction.

Table 1. Extreme Precipitation Indices

Abbreviation	Name	Description
PRCPTOT	Annual total wet-day precipitation	Total annual precipitation from days with ≥1 mm rainfall
SDII	Simple daily intensity index	Ratio of total precipitation (≥1 mm) to the number of wet days
R95P	Very wet days precipitation	Total precipitation from days exceeding the 95th percentile threshold
R99P	Extremely wet days precipitation	Total precipitation from days exceeding the 99th percentile threshold
RX1DAY	Maximum 1-day precipitation	Highest 1-day precipitation amount within a given period
RX3DAY	Maximum 3-day precipitation	Highest consecutive 3-day precipitation amount within a given period

3.3. Trend and Change-Point Detection Methods

This study employs three trend analysis methods - the least squares method, Mann-Kendall (M-K) trend test, and Spearman's rank trend test - to determine precipitation variation characteristics in the Chaohu Lake Basin. The least squares trend analysis method fits a linear regression to the data series using ordinary least squares, where the slope of the fitted line represents the trend magnitude. The M-K trend test is a non-parametric method for identifying monotonic trends in time series data that does not require normal distribution assumptions and is robust to missing values and outliers (Koycegiz et al, 2024). Spearman's rank trend test evaluates the significance of the correlation coefficient between the ranks of hydro-meteorological series and time to determine trend existence (Tuğrul and Hinis, 2024).

Following the multi-stage change-point detection framework (Niu et al, 2021, Zhang et al, 2025), the analysis process consists of four steps: preliminary diagnosis, detailed diagnosis, comprehensive diagnosis, and final conclusions. Preliminary diagnosis utilizes the Hurst exponent to estimate overall variation characteristics. The Hurst exponent (H) ranges from 0 to 1, where: 1) H = 0.5 indicates a random walk time series with no autocorrelation; 2) H > 0.5 suggests positive autocorrelation with persistent trends; 3) H < 0.5 indicates negative autocorrelation with mean-reverting tendencies. Detailed diagnosis employs five change-point localization methods: 1) M-K change-point test; 2) Moving t-test; 3) Lee-Heghinian test; 4) Ordered clustering method; 5) Optimal information partitioning method. Comprehensive diagnosis integrates results from all detailed diagnostic methods. Combined with preceding trend analysis outcomes, final conclusions are drawn regarding change-point detection. An overview of all the trend and change-point detection methods used in this study is provided in Table 2.

Table 2. Trend and Change-Point Detection Methods

Diagnosis Type	Methods
Trend Analysis	Least squares method
	M-K trend test
	Spearman's trend test
Change-Point Detection	Hurst exponent method
	M-K change-point test
	Moving t-test
	Lee-Heghisnian Test
	Ordered clustering method
	Optimal information partitioning method

3.4. Probability Distribution Change Detection Method

In the field of hydrological and water resources research, commonly used univariate independent marginal distributions include the Generalized Extreme Value (GEV) distribution, Pearson Type III distribution, and log-normal distribution. This study selects the GEV distribution as the marginal distribution fitting function for precipitation in the Chaohu Lake Basin. The marginal distributions are fitted separately for the baseline period and variation period to analyze characteristic changes before and after the change-point. To comprehensively consider whether interannual variations and flood season patterns are consistent, separate analyses are conducted for annual averages and June-September monthly average series.

The Generalized Extreme Value distribution function is expressed as:

$$P(x) = \begin{cases} \frac{1}{\sigma}\exp\left(-\left(1+k\frac{x-\mu}{\sigma}\right)^{-1/k}\right)\left(1+k\frac{x-\mu}{\sigma}\right)^{-1-1/k} & k \neq 0 \\ \frac{1}{\sigma}\exp\left(-\frac{x-\mu}{\sigma}-\exp\left(-\frac{x-\mu}{\sigma}\right)\right) & k = 0 \end{cases} \tag{1}$$

Where: P is fit the theoretical probability; $\boldsymbol{\mu}$ is logarithmic mean of the sample; $\boldsymbol{\sigma}$ is logarithmic mean square error of the sample; k is shape coefficient of the sample. Correspondingly, the fitting parameters of the generalized extreme value distribution function are logarithmic mean, logarithmic mean square error and shape coefficient.

3.5. Statistical Analysis and Software

All statistical analyses and graphical visualizations were accomplished using the MATLAB programming environment (MATLAB R2024a). Specifically, the calculation of extreme precipitation indicators was carried out using a self-written program; trend analysis and abrupt change analysis were conducted using the built-in function libraries of MATLAB and post-processing was carried out by self-written code; the generalized extreme value distribution (GEV) was fitted using the marginal distribution function in the "Copula" package. The author combined these four parts into a unified tool, thereby implementing the Trend-Mutation-Probability (TMP) diagnostic framework.

4. Results and Discussion

4.1. General Precipitation Trends and Extreme Precipitation Evolution in the Chaohu Lake Basin

Figure 3 illustrates the interannual variations in precipitation across the Chaohu Lake Basin, including annual and flood-season (June–September) precipitation, along with the spatial distribution of the 15 monitoring stations. The results indicate that the long-term average annual precipitation in the basin is 1,176 mm. The lowest precipitation years were 1966 and 1978, with annual totals of 743 mm and 308 mm, respectively, and corresponding flood-season precipitation of 607 mm and 231 mm. The mean flood-season precipitation was 602 mm, accounting for 51.2% of the annual total, with the lowest values again occurring in 1966 and 1978. Spatially, precipitation distribution during dry years showed relatively uniform station-to-station variability, with a range of approximately 500 mm. In contrast, wet years exhibited greater spatial heterogeneity, with some stations experiencing extreme precipitation events. The largest inter-station difference occurred in 1969, with a maximum discrepancy of 1,176 mm between the wettest and driest stations. That year recorded an annual precipitation of 1,462 mm and flood-season precipitation of 1,062 mm.

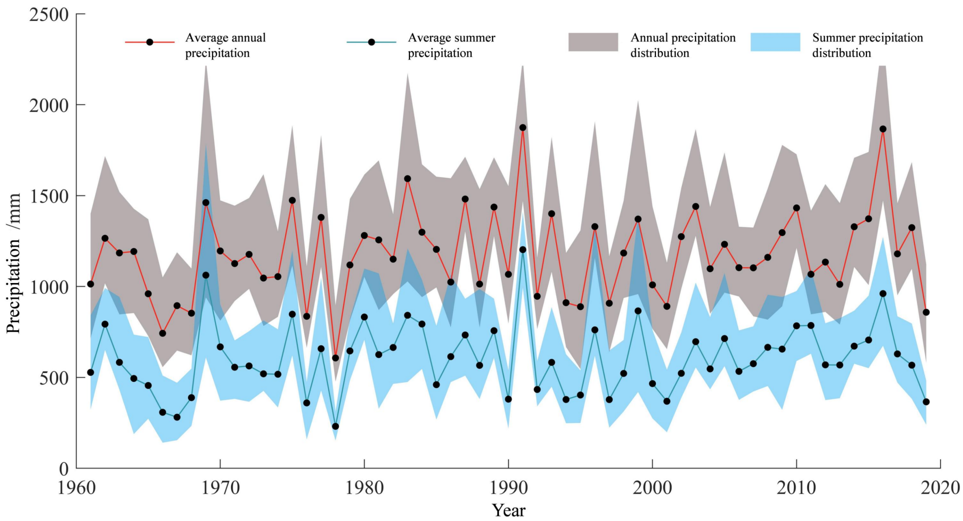

Figure 3. Interannual variations in annual and flood-season precipitation, along with their spatial distribution across monitoring stations.

Figure 4 presents the interannual trends and spatial distribution of extreme precipitation indices. The fitted curves indicate an overall increasing trend for all six indices, with the most pronounced rise observed in the annual wet-day precipitation total (PRCPTOT). In contrast, the simple daily intensity index (SDII) and the maximum 1-day precipitation (Rx1day) exhibited the weakest upward trends. Collectively, these results suggest an increasing frequency of extreme precipitation events in the Chaohu Lake Basin. Spatially, the variability in PRCPTOT, SDII, heavy precipitation (R95p), and very heavy precipitation (R99p) closely mirrored the patterns of annual and flood-season precipitation, with greater fluctuations observed in years of higher total precipitation. In contrast, the spatial variability of Rx1day and the maximum 3-day precipitation (Rx3day) showed weaker correlations with precipitation magnitude.

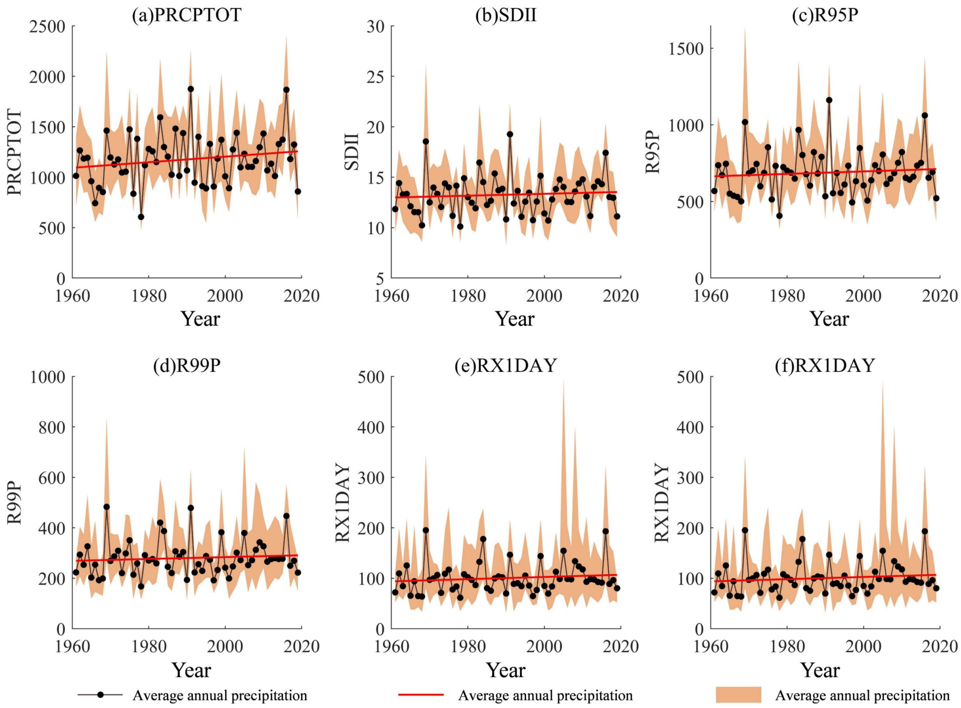

Figure 4. Interannual trends of extreme precipitation indices and their spatial distribution.

4.2. Analysis of Precipitation Trend Evolution in Chaohu Lake Basin

Table 3 presents the trend analysis results for annual and flood-season precipitation, while Figure 5 displays their spatial distribution patterns. The results show that the station-averaged annual precipitation trends derived from least squares, Mann-Kendall test, and Spearman's test were 2.4, 2.0, and 1.1 respectively, with corresponding flood-season values of 1.2, 1.5, and 1.1, indicating statistically significant increasing trends. Notably, the increasing trend was more pronounced for annual precipitation than for flood-season precipitation. Among the 15 rainfall stations, 14 exhibited trends consistent with the station average, with only Feixi Station (No. 3) showing a decreasing trend. Spatially, the increasing trends were more substantial in peripheral areas of the basin compared to central regions, except for Feixi Station.

Table 3. Trend analysis results of annual and flood-season precipitation

Precipitation station number	Annual precipitation			Flood season precipitation		
	Least squares method	M-K	Spearman	Least squares method	M-K	Spearman
1	3.5	3.5	1.7	2.2	2.6	1.7
2	3.1	2.7	1.3	1.8	2.4	1.2
3	-3.2	-2.7	-1.4	-2.7	-1.5	-1.1
4	3.6	3.1	1.8	2.2	2.4	1.6
5	3.7	3.5	2.2	2.2	2.8	1.7
6	5.0	4.4	2.8	3.1	2.4	2.3
7	2.4	1.5	1.0	1.4	1.2	0.7
8	2.3	1.5	0.8	1.3	1.7	1.0
9	2.4	1.5	0.6	0.6	0.7	0.3
10	3.3	3.3	1.4	2.1	2.0	1.2
11	3.7	3.6	1.4	2.1	1.4	1.2
12	1.8	1.7	1.0	0.6	0.9	0.5
13	2.6	3.3	1.5	0.6	1.2	0.7
14	2.0	1.7	0.8	0.4	0.5	0.2
15	5.1	4.0	2.0	2.7	2.5	1.2
Mean across stations	2.4	2.0	1.1	1.2	1.5	1.1

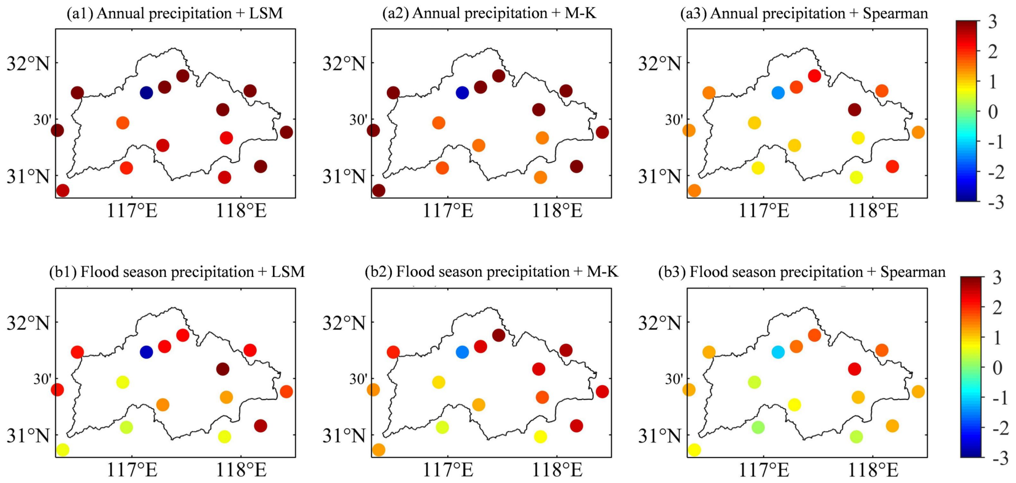

Figure 5. Spatial distribution of annual and flood-season precipitation trends

Table 4 presents the trend analysis results for six extreme precipitation indices. The station-averaged analysis revealed that the annual wet-day precipitation total (PRCPTOT) showed the most significant increasing trend, with least squares, Mann-Kendall, and Spearman's test values of 2.4, 2.0, and 1.1 respectively, followed by heavy precipitation (R95p) with corresponding values of 0.8, 0.9, and 0.9. In contrast, the simple daily intensity index (SDII), very heavy precipitation (R99p), maximum 1-day precipitation (Rx1day), and maximum 3-day precipitation (Rx3day) exhibited non-significant increasing trends. It should be noted that SDII values from least squares and Mann-Kendall tests approached zero, consistent with the earlier conclusion from Figure 4 that SDII showed no significant increasing trend.

Figure 6 illustrates the spatial distribution of extreme precipitation index trends. The results clearly demonstrate increasing trends for PRCPTOT and R95p, which align with the observed patterns in annual and flood-season precipitation trends. Again, the magnitude of change was greater in peripheral areas than in central regions. While SDII showed virtually no change, R99p, Rx1day, and Rx3day maintained non-significant increasing trends.

Table 4. Trend analysis of extreme precipitation indices

Extreme precipitation indices	Least squares method	M-K	Spearman
PRCPTOT	2.4	2	1.1
SDII	0	0	1.8
R95P	0.8	0.9	0.9
R99P	0.2	0.2	0.6
RX1DAY	0.2	0.1	1.1
RX3DAY	0.2	0.3	0.9

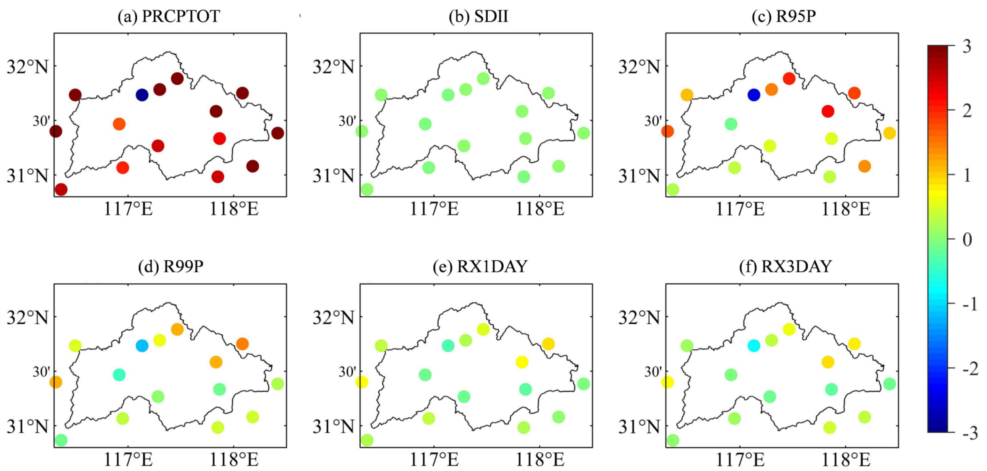

Figure 6. Spatial distribution of extreme precipitation index trends

4.2. Abrupt Change Analysis of Precipitation in Chaohu Lake Basin

Table 5 presents the results of the abrupt change diagnosis for annual and flood-season precipitation in Chaohu Lake Basin. The diagnostic procedure consisted of four sequential steps:

First, preliminary diagnosis was conducted. The Hurst indices for annual and flood-season precipitation were 0.52 and 0.55, respectively. Since Hurst > 0.5 indicates positive autocorrelation in the time series with persistent trends, both annual and flood-season precipitation exhibited weak variability.

Second, detailed diagnosis was performed using five methods: the Mann-Kendall abrupt change test, moving t-test, Lee-Heghinian test, ordered clustering method, and optimal information segmentation method to identify multiple potential change points. For annual precipitation, all methods except the moving t-test detected 1979 as the change point. For flood-season precipitation, the moving t-test again failed to detect any change point, while the Mann-Kendall test identified 1979 and 1990 as change points. Both the Lee-Heghinian test and ordered clustering method identified 1968, and the optimal information segmentation method identified 1982 as change points.

Third, comprehensive diagnosis was conducted. For annual precipitation, four methods consistently identified 1979 as the sole change point, thus confirming 1979 as the definitive abrupt change year. For flood-season precipitation, two methods identified 1968 as the primary change point without consensus among other methods, leading to 1968 being designated as the comprehensive change point.

Fourth, diagnostic conclusions were drawn. Combined with trend analysis results, both annual and flood-season precipitation series exhibited significant abrupt changes, with pronounced increasing trends observed both before and after the change points.

Table 5. Results of abrupt change diagnosis for annual and flood-season precipitation in Chaohu Lake Basin

Diagnostic Procedure	**Method**	**Annual Precipitation**	**Flood-Season Precipitation**
Preliminary Diagnosis	Hurst Exponent	0.52	0.55
	Overall Variability Level	Weak persistence	Weak persistence
Detailed Diagnosis	Mann-Kendall Abrupt Change Test	1979	1979/1990
	Moving t-test	/	/
	Lee-Heghinian Test	1979	1968
	Ordered Clustering Method	1979	1968
	Optimal Information Segmentation	1997	1982
Comprehensive diagnosis		1979(3+)	1968(2+)
Diagnostic conclusions		Abrupt change Significant increasing trend	Abrupt change Significant increasing trend

4.4. Precipitation Distribution Characteristics Before and After Abrupt Changes in Chaohu Lake Basin

Based on the previously identified change points, the precipitation series were divided into pre- and post-abrupt change periods. Using 1979 as the change point for annual precipitation, Figure 7 presents the marginal distribution functions of annual precipitation across Chaohu Lake Basin before and after the abrupt change.

Figure 7(a) reveals a rightward shift in the post-change precipitation distribution across all frequencies, particularly pronounced at $P<0.1$ and $P>0.9$ where precipitation increased by over 100 mm. The divergence progressively widens at $P>0.9$, indicating significantly enhanced extreme precipitation events at the basin scale following the regime shift. Figure 7(b) shows the marginal distribution functions for Feixi Station, where annual precipitation generally decreased post-change. While dry-year precipitation ($P>0.9$) remained largely unchanged, substantial reductions (exceeding 200 mm at $P=0.9$) occurred in wetter years. Notably, all 14 other hydrologic stations exhibited distributional changes consistent with the basin-average pattern (not shown).

Figure 8 displays the flood-season precipitation marginal distribution functions before and after the abrupt change (1968). While generally similar to annual precipitation patterns, key differences emerge due to the differing change points. For instance, Figure 8(b) shows intersecting distribution curves at $P=0.85$ for Feixi Station, with post-change decreases at $P<0.85$ but increases at $P>0.85$ - a pattern contrasting with annual precipitation. This discrepancy likely stems from the earlier change point (1968), where the pre-change flood-season series had only 8 degrees of freedom.

To facilitate comparison, Table 6 provides: (1) precipitation values at key frequencies, and (2) precipitation differences between pre- and post-change periods.

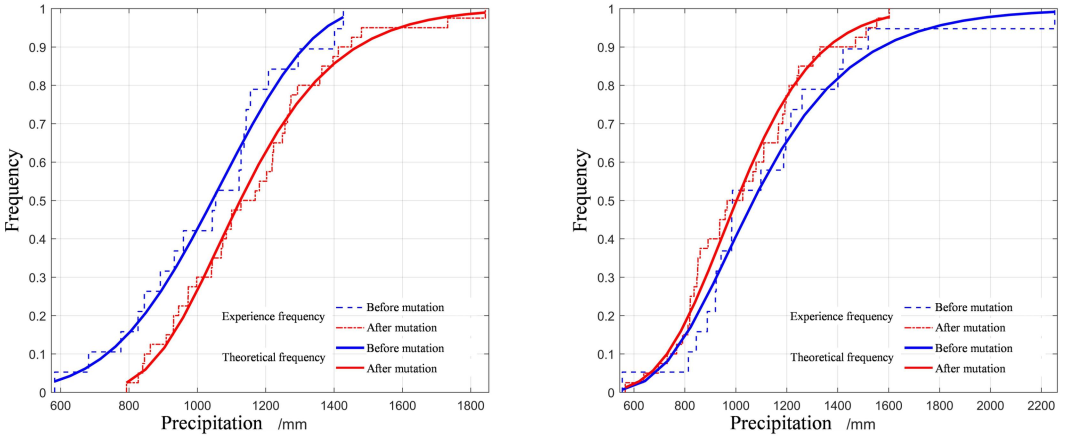

(a)Basin-average (b)Feixi Station

Figure 7. Marginal distribution functions of annual precipitation in Chaohu Lake Basin before and after the abrupt change point

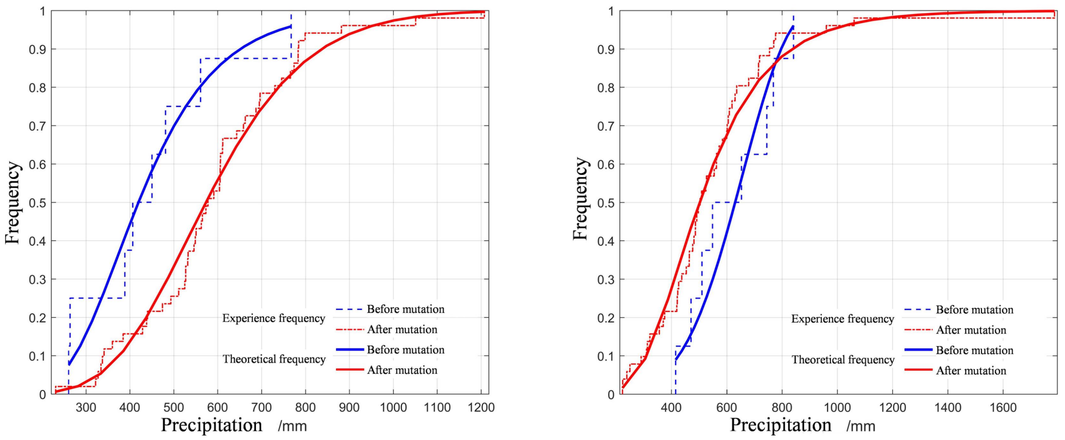

(a)Basin-average (b)Feixi Station

Figure 8. Marginal distribution functions of flood-season precipitation in Chaohu Lake Basin before and after the abrupt change point

Table 6. Parameter estimates of marginal distributions for annual precipitation in Chaohu Lake Basin before and after the abrupt change point (1979).

Station	**Period**	**Probability**								
		P=0.1	**P=0.2**	**P=0.3**	**P=0.4**	**P=0.5**	**P=0.6**	**P=0.7**	**P=0.8**	**P=0.9**
stations average	Before mutation	739.9	845.8	922.1	986.7	1046.1	1104.2	1160.8	1227.5	1311.3
	After mutation	890.9	962.5	1019.7	1072.8	1125.3	1182.9	1249.5	1334.5	1465.9
	Precipitation difference	151.0	116.7	97.6	86.1	79.2	78.7	88.7	107.0	154.6

4.5. Potential Driving Mechanisms: Insights from Teleconnections and Urbanization

Teleconnections: We now link the identified abrupt change point (1979) to the well-documented late-1970s global climate shift, particularly the phase change of the Pacific Decadal Oscillation (PDO). We propose a plausible pathway: PDO phase change → modulation of the Western Pacific Subtropical High → altered moisture transport → modified precipitation regimes in the basin. This connects our regional finding to decadal climate variability.

Urbanization: We provide an in-depth interpretation of the spatial pattern where peripheral stations show more significant increases. We hypothesize that this could be attributed to urban heat island effects from cities like Hefei, potentially enhancing convective precipitation downwind.

5. Conclusions

This study presents a quantitative analysis of extreme precipitation evolution characteristics in the Chaohu Lake Basin through extreme precipitation indices, trend diagnostics, abrupt change detection methods, and comparative analysis of marginal distribution curves. The principal findings are as follows:

(1) Both annual and flood-season precipitation exhibited statistically significant increasing trends across the basin, with the most pronounced trends observed at peripheral stations. Precipitation heterogeneity among stations increased with precipitation magnitude—the maximum inter-station difference reached 1,176 mm in 1969 (annual precipitation: 1,462 mm; flood-season precipitation: 1,062 mm). Among extreme precipitation indices, the annual wet-day precipitation total (PRCPTOT) showed the most marked increase, though all five indices demonstrated rising trends.

(2) The abrupt change point for annual precipitation occurred in 1979, consistently identified by four diagnostic methods (excluding the moving t-test). For flood-season precipitation, 1968 was detected as the change point by both the Lee-Heghinian test and ordered clustering method.

(3) Post-abrupt change analysis revealed rightward shifts in the marginal distributions of station-averaged annual precipitation across all quantiles, particularly exceeding 100 mm increases at $P<0.1$ and $P>0.9$. The divergence amplified progressively at $P>0.9$, indicating significantly enhanced extreme precipitation events at the basin scale. Notably, Feixi Station showed decreasing trends post-change, while all other stations exhibited increases—a pattern mirrored in flood-season precipitation.

(4) This study quantitatively reveals extreme precipitation evolution in the Chaohu Lake Basin. The quantified increase, particularly over 100 mm at high quantiles, provides critical evidence for updating flood control standards in the Yangtze River Delta. The long-term data and detected shifts serve as a vital benchmark for validating regional climate models over urbanizing terrains. Furthermore, the basin's "drought-flood alternation" under compound pressures offers a significant comparative case for international water security studies.

This study is limited by the density of observation sites and the uncoupled land use data. In the future, it is necessary to combine high-resolution climate-hydrology coupled models to enhance the predictive ability. The 'cloud seeding - urbanization' game phenomenon in the Chaohu Lake Basin also provides a comparable sample for similar rapidly developing areas worldwide.

Author Contributions

All authors were involved in designing and discussing the study. ZHANG Ye, WANG Leizhi and HU Jianwen undertook the data analysis and drafted the manuscript; ZHU Wei collected the required data; TIAN Dan and WU Lei revised the manuscript and edited the language; DENG Pengxin contributed to the set-up of the simulations and the writing of the paper. All authors have read and agreed to the submitted version of the manuscript.

Funding

This work was supported by the National Natural Science Foundation of China (Grant No.52309026; 52239008); the Science and Technology Project of Power Construction Corporation of China (Grant No. E001Y240006); the Postgraduate Thesis Foundation of Nanjing Hydraulic Research Institute (Grant No. Yy525013); the Key Laboratory of Digital Twin Basin, Ministry of Water Resources (Grant No. KLRBDT202504); and the Central Level Public Welfare Scientific Research Institutes Fundamental Research Funds (Grant No. Yj526015; Yj526001).

Conflicts of Interest

The authors declare no conflict of interest.

References

Ayugi B, Dike V, Ngoma H, et al. Future changes in precipitation extremes over East Africa based on CMIP6 models[J]. Water, 2021, 13(17): 2358. https://doi.org/10.3390/w13172358

Du H, Donat MG, Zong S, et al. Extreme Precipitation on Consecutive Days Occurs More Often in a Warming Climate[J]. Bulletin of the American Meteorological Society,2022, 103(4):1130-1145. https://doi.org/10.1175/BAMS-D-21-0140.1

Du Junkai, Qiu Yaqin, Du Junkai, et al. Evolution characteristics of the interannual and intra-annual precipitation in China from 1956 to 2016 [J]. Advances in Water Science, 2023, 34(2):182-196. https://dx.doi.org/10.14042/j.cnki.32.1309.2023.02.003

Franzke CLE. Changing temporal volatility of precipitation extremes due to global warming[J]. International Journal of Climatology,2022,42(16):8971-8983. https://doi.org/10.1002/joc.7789

Guo J, Shen Y, Wang X, et al. Evaluation and projection of precipitation extremes under 1.5°C and 2.0°C GWLs over China using bias-corrected CMIP6 models[J]. Iscience, 2023, 26(4):106179. https://doi.org/10.1016/j.isci.2023.106179

He Jia, Su Xiao. Research Progress on Extreme Climate Events and Evolution of Major Disasters [J]. Disaster science,2018,33(04):223-228. https://doi.org/10.3969/j.issn.1000-811X.2018.04.038

IPCC. Climate Change 2022: impacts, adaptation, and vulnerability[M]. Cambridge: Cambridge University Press, 2022. https://doi.org/10.1017/9781009325844

Koycegiz C. Spatiotemporal analysis of precipitation variability in an endorheic basin of Turkey with coordinated regional climate downscaling experiment data[J]. Alexandria Engineering Journal, 2024, 91: 368-381. https://doi.org/10.1016/j.aej.2024.02.010

Liu S, Huang S, Huang Q, et al. Identification of the non-stationarity of extreme precipitation events and correlations with large-scale ocean-atmospheric circulation patterns: A case study in the Wei River Basin, China[J]. Journal of Hydrology, 2017, 548:184-195. https://doi.org/10.1016/j.jhydrol.2017.03.012

Niu K, Hu Q, Wang Y, et al. Analysis on the Variation of Hydro-Meteorological Variables in the Yongding River Mountain Area Driven by Multiple Factors[J]. Remote Sensing, 2021, 13(16): 3199. https://doi.org/10.3390/rs13163199

Tang Q. Global change hydrology: Terrestrial water cycle and global change[J]. Science China-Earth Sciences,2020,63(3):459-462. https://doi.org/10.1007/s11430-019-9559-9

Teegavarapu R, Nayak A. Evaluation of long-term trends in extreme precipitation: Implications of in-filled historical data use for analysis[J]. Journal of Hydrology, 2017, 550. https://doi.org/10.1016/j.jhydrol.2017.05.030

Tuğrul T, Hinis M A. Trend analysis of hydrological and meteorological drought in Apa Dam, Türkiye[J]. Environmental Earth Sciences, 2024, 83(17): 502. https://doi.org/10.1007/s12665-024-11791-z

Tysa S K, Ren G, Zhang P, et al. Impact of urbanization on regional extreme precipitation trends observed at China national station network[J]. Weather and Climate Extremes, 2025, 48: 100760. https://doi.org/10.1016/j.wace.2025.100760

Wu F, Yang X, Cui Z, et al. The impact of human activities on blue-green water resources and quantification of water resource scarcity in the Yangtze River Basin[J]. Science of the Total Environment, 2024, 909: 168550. https://doi.org/10.1016/j.scitotenv.2023.168550

Xing S, Li X. Diurnal variation of global precipitation: an analysis of CMORPH data[J]. Journal of Tropical Meteorology,2019,25(1):45-53. https://doi.org/10.16555/j.1006-8775.2019.01.005

Xu Xiaolu, Zhang Fangmin, Deng Hanqing, et al. Changes in Precipitation Grades in China from 1961-2020 [J]. Research of Soil and Water Conservation,2024,31(2):181-189. https://doi.org/10.13869/j.cnki.rswc.2024.02.003

Zhang Cunjie, Xiao Chen, Li Shuai, et al. Construction of multi-extreme climate events composite grads index and comprehensive analysis of extreme climate in the Yangtze River Basin from 1961 to 2020 [J]. Journal of Geophysics,2023,66(3):920-938. https://doi.org/10.6038/cjg2022Q0255

Zhang S, Xu Q, Riffat S. Multi-objective optimization on sustainable retrofit of historical buildings using NSGA-II Algorithm: A case study of Suzhou[J]. Green Technology & Innovation, 2025: 7658. https://dx.doi.org/10.36922/gti.7658

Zhang W, Liu L, Li X, et al. Intensified response of extreme precipitation to rising temperature over the Tibetan Plateau from CMIP6 multi-model ensembles[J]. Journal of Hydrology, 2024, 637: 131397. https://doi.org/10.1016/j.jhydrol.2024.131397

Zhang Y, Wang K. Global precipitation system scale increased from 2001 to 2020[J]. Journal of Hydrology,2023,616:128768. https://doi.org/10.1016/j.jhydrol.2022.128768

Zhao L, Li L, Li Y, et al. Global extreme precipitation characteristics: the perspective of climate and large river basins[J]. Climate Dynamics,2024,62(2):1013-1030. https://doi.org/10.1007/s00382-023-06961-x